Carbohydrate Polymers 74 (2008) 290–300

Contents lists available at ScienceDirect

Carbohydrate Polymers

journal homepage: www.elsevier.com/locate/carbpol

Preparation and characteristics of moulded biodegradable cellulose fibers/MPU-20 composites (CFMCs) by steam injection technology

Detao Liu *, Jun Li, Rendang Yang, Lihuan Mo, Lianghui Huang, Qifeng Chen, Kefu Chen

Guangdong Public Laboratory of Paper Technology and Equipment, South China University of Technology, Guangzhou 510640, China
State Key Laboratory of Pulp and Paper Engineering, South China University of Technology, Guangzhou 510640, China

ARTICLE INFO

Article history:
Received 22 October 2007
Received in revised form 25 January 2008
Accepted 28 February 2008
Available online 6 March 2008

Keywords:
Cellulose fibers/MPU-20 composites (CFMCs)
Self-designed steam injection technology and equipment
Cushioning properties
Physicochemical characteristics

ABSTRACT

In this work, the moulded cellulose fibers/MPU-20 composites (CFMCs) with apparent specific gravity lower than 100 kg/m^3 and thickness of 20–200 mm have been successfully manufactured using a new design of steam injection technology and equipment. It was found that the CFMCs have good cushioning properties, with a cushion factor lower than 4. Two yield deformation stages were observed in the compressive process. Compressive stress–strain and cushion factor-stain curves were measured as a function of steam injection pressure, transmission time, holding time, MPU-20 resin dosage and apparent specific gravity. Chemical groups, crystallinity, and thermal properties of samples were studied through the use of FTIR spectroscopy, X-ray diffraction (XRD), and DTA–TGA. In addition, the microstructure and morphology were investigated by scanning electron microscope (SEM) and atomic force microscope (AFM).

1. Introduction

Loose-filled packaging materials (e.g. expanded polystyrene (EPS) and expanded polyethylene (EPE) can provide cushioning, protection, and stabilization of packaged articles for shipping (Tatarka & Cunningham, 1998). However, the widespread use of the present packaging materials is under growing pressure from existing and proposed environmental and disposal regulations related to concerns with biodegradable and solid waste management (Mugnozza et al., 2006; Steinbüchel, 1992; Tatarka & Cunningham, 1998; Yogaraj & Ramani, 2006). Many countries have or are considering legislations for limiting the use of EPS and EPE as packaging materials. These actions are a part of a larger effort to produce environmentally friendly alternatives which are biodegradable (Lui & Peng, 2007). Such as starch-based biodegradable materials (Avella et al., 2005; Guan, Eskridge, & Hanna, 2005; Vox & Schettini, 2007), and moulded pulp materials (Chang & Hung, 2003; Noguchi, Miyashita, Seto, Tan, & Kawano, 1997).

Cellulose plant fibers, as the most abundant renewable and biodegradable resource on the planet, have extraordinary potential for industrial applications. The cellulose plant fibers have the advantages of low apparent specific gravity, low cost, recyclability and biodegradability (Bourmaud & Baley, 2007; Mohanty, Wibowo, Misra, & Drzal, 2004; Voorn, Smit, Sinke, & Klerk, 2001). Therefore, it is desired to utilize cellulose plant fibers in the production of loose-filled cushion materials. However, composites (e.g. Corrugated board, fiberboard, particleboard) consisting of cellulose fibers bonded together with a synthetic resin under heat and pressure, usually have higher apparent specific gravities as a consequence of the need for greater rigidities and reduced cushion properties due to the comparatively fewer voids in structure. There are previous reports on low-density composites bonded with isocyanate resin that were fabricated by steam injection pressing (Hata, 1993; Kawasaki, Zhang, & Kawai, 1998), however, these composites had poor cushioning properties due to relative higher apparent specific gravities, and were mainly used as building materials or light-weight core materials instead of being used as cushioning materials.

To overcome these problems, we were interested in preparing the cellulose fibers/MPU-20 composites (CFMCs) with good cushioning properties using a new design of steam injection technology and equipment. The static compression and the physicochemical properties of the CFMCs were evaluated as a function of steam injection pressure, transmission time, holding time, MPU-20 resin dosage, and apparent specific gravity.

* Corresponding author. Address: Guangdong Public Laboratory of Paper Technology and Equipment, South China University of Technology, Guangzhou 510640, China. Tel.: +86 15918749518; fax: +86 02087114105.
E-mail address: liudetao2003@126.com (D. Liu).

0144-8617/$ - see front matter © 2008 Elsevier Ltd. All rights reserved.
doi:10.1016/j.carbpol.2008.02.015

2. Materials and methods

2.1. Experimental equipment design and manufacture

The experimental equipment for preparation of the CFMCs (as shown in Fig. 1) used in this work was designed and constructed especially for this study. The piston-type former is shown in detail in Fig. 2 and consists of an upper pore plate and an under pore plate. As can be seen in this figure, the equipment consists of piston-type former, steam generator and other accessories. A large number of 3 mm diameter spray-holes, spaced 6 mm apart, were drilled in the pore plates to permit steam flow. In the process, steam with maximum injection pressure of 700 kPa was generated from the steam generator and flowed along the pipes. When the steam reached the former, it quickly moved through the porous cellulose fibers/MPU-20 blends driven by the external pressure gradients in a very short time.

2.2. Materials and chemicals

The cellulose fibers samples (Pine fibers) used in the laboratory trials were kindly supplied by Jiangxi Oasis Wood-based Panels Co., Ltd. (Jiangxi, China) and were prepared using a pressurized disc refiner. The initial moisture content of the cellulose fibers was about 10%. The foam-type MPU-20 of polyurethane resin was purchased from Jingjiang City Specific Adhesive Factory (Jiangsu, China) with apparent specific gravity of 50 kg/m^3 and dynamic viscosity of 8–20 pa.s. The acetone or ethyl acetate was purchased from Jingke Chemical Agents & Glass Instrument Wholesale Department (Guangdong, China) and was used as the solvent to dilute the resin so that it could be more easily mixed with the cellulose fibers. The steam generator was purchased from Shanghai Huazheng Thermal Equipments Co., Ltd. (Shanghai, China). The Micro Air Compressing Engine was purchased from Taizhou Sanhe Mechanical Co., Ltd. (Zhejiang, China).

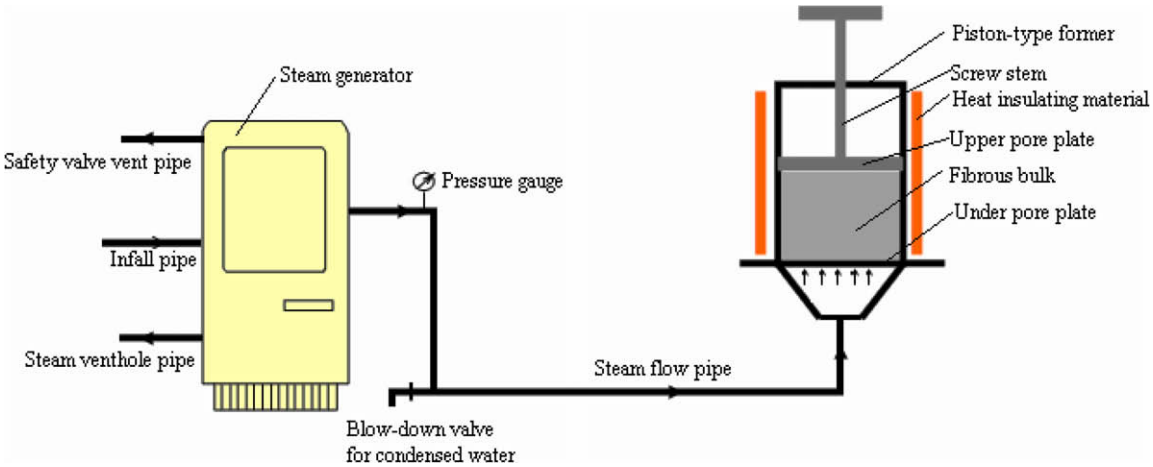

Fig. 1. Schematic of molding process for the CFMCs by steam injection technology.

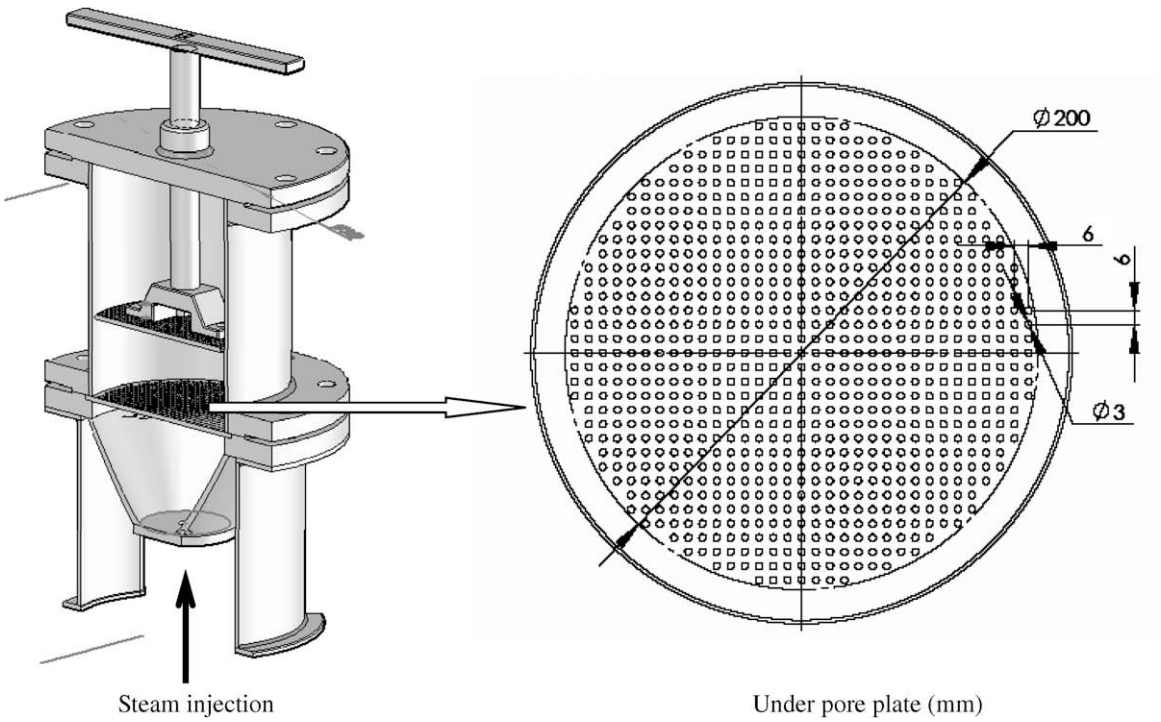

Fig. 2. The detailed structural schematic for piston-type former.

2.3. Preparation of the CFMCs

Before the laboratory trials, the cellulose fibers were screened through a 10 × 10 mm sieve to remove the larger fibrous-mass. The MPU-20 resin was dissolved in acetone or ethyl acetate. Subsequently, the diluted MPU-20 resin was poured into the tank of the spray pistol, which was linked to the Micro Air Compressing Engine. A certain amount of cellulose fibers were filled in a sealed plastic sack with a small hole.

When the trial started, the spray nozzle of the spray pistol was inserted into the plastic sack through the small hole. As the compressing engine was working, the spray pistol produced a strong airflow, which created a Venturi vacuum that caused the introduction of MPU-20 resin/solvents mixtures into the airflow. In this procedure, the atomized MPU-20 resin particles from spray nozzle were well mixed with the dispersed cellulose fibers inside the plastic sack. After the mixing of the cellulose fibers with MPU-20 resin, the blends were rapidly poured into the main forming zone of the piston-type former.

Then the steam generator began supplying steam, which flowed along the pipes and subsequently moved through the porous cellulose fibers/MPU-20 blends due to the outer pressure gradients. After the objective transmission time used in trials, the steam injection was terminated, and after a specific holding time, the porous blends was released from the former and air-dried for 24 h.

2.4. Mechanical testing

Static compression tests were carried out at room temperature of 20 °C and relative humidity of 60%, using a computerized universal testing machine operated at a speed of 12 mm/min. The tests included both compressive stress-strain and cushion factor-strain evaluations under static compression. The test samples were moulded and formed under different steam injection pressures, holding times, transmission times, MPU-20 resin dosages and apparent specific gravities. MPU-20 resin dosage was calculated from the ratio of pure resin liquid weight to total oven-dried cellulose fibers weights of the CFMCs sample. Penetration time was defined as the time from the beginning of steam application to the appearance of steam through a small hole on the upper-side of the former, and transmission time was defined as the time from the appearance of this steam to the cessation of the steam injection process. Finally, the holding time was defined as the time from the cessation of the steam injection to the release of the sample from the former.

2.5. SEM analysis

Samples of air-dried cellulose fibers were fixed to a metal-base specimen holder using double-sided sticky tape. Thin-film samples of the air-dried CMFCs were sliced using a shape-edged razor. These samples were also fixed to a metal-base specimen holder with double-sided sticky tape. The samples of cellulose fibers and the CMFCs were coated with gold using a vacuum sputter-coater. The fracture surfaces were observed in a scanning electron microscope (SEM) Model using a Philips XL-30 ESEM after the samples were gold coated.

2.6. AFM analysis

Atomic Force Microscopy (AFM) analysis was conducted in order to observe the morphology of the cellulose fibers surfaces using a Veeco Di Multimode SPM instrument, AFM scanning was carried out in air by contact AFM mode, and the other conditions were; tip radius of curvature 10–20 nm, scanning rate of 0.2999 Hz, scan size of 5.000 μm and data scale of 100.0 nm.

2.7. FTIR analysis

FTIR analyses were performed in a Thermo Nicolet Nexus 470 FTIR spectrophotometer using a standard KBr pellet technique. Each spectrum was recorded with 32 scans in the frequency range from 4000 to 400 cm^{-1} with a resolution of 4 cm^{-1}.

2.8. XRD analysis

X-ray diffraction (XRD) analyses of the cellulose fibers blends untreated and treated by steam injection treatment, and the CFMCs were carried out using an X-ray diffraction analyzer (Model No: Rigaku D/max-III A X-ray diffractometer) at 40 kv and 30 mA. Wide-angle X-ray intensities were collected for 2θ ranging from 4° to 60° with step scanning rate of 8°/min and step length of 0.04°.

2.9. DTA–TGA analysis

For thermoanalytical studies, using a NETZSCH STA 449 C Jupiter Thermal Analysis System that combined DTA and TGA measurements, were conducted. Differential thermal analysis (DTA) measurements were performed with 2.25 mg samples at a heating rate of 10 °C min^{-1} in an oxygen atmosphere. Thermogravimetric analysis (TGA) was used to study the thermal stability. The weight loss was recorded in the range from room temperature to 500 °C with a heating rate of 10 °C min^{-1}.

3. Results and discussion

3.1. FTIR spectral analysis

The nature of chemical bonding between cellulose fibers and MPU-20 was investigated by FTIR spectroscopy (as shown in Fig. 3). FTIR spectrum for MPU-20 showed a broad band around 2270 cm^{-1} that was attributable to isocyanate groups; i.e. —NCO. FTIR spectrum for the CFMCs showed that the C=O stretching vibration peak, corresponding to that of urethane (—NH—CO—O—), appeared at absorption 1721 cm^{-1}, and the —NCO of isocyanate band at 2270 cm^{-1} is nearly disappeared. These data suggest the formation of urethane (—NH—CO—O—) as a result of the chemical reaction between —NCO groups from MPU-20 and —OH groups from cellulose fibers (Karmarkar, Chauhan, Modak, & Chanda, 2007; Silva, Martínez, & Bordado, 2006). The CH_2 sym bending pyran cycle at 1467 cm^{-1} was attributable to a degraded low molecular weight polyoses from semi-cellulose in the cellulose fibers blends subjected to steam injection treatment (Gironès et al., 2007; Widyorini, Xu, Watanabe, & Kawai, 2005). Other important bands for the CFMCs were located in the wide band centered at 3403 cm^{-1}. These features are probably mixed peaks resulting from free N—H stretching vibration in urethane and/or —OH stretching in cellulose and water. The peak at 1420 cm^{-1} indicated the absorption peak by the C—N amide group in urethane. Likewise, the 1220 cm^{-1} peak was attributed to Ar—NH—COO— in urethane, which indicated that there was probably also a benzene structure at least in the MPU-20 resin (Tejado et al., 2007). Based on spectral evidences and previous literatures (Das, Malmberg, & Frazier, 2007; Hata, 1993; Karmarkar et al., 2007; Kawasaki et al., 1998; Silva et al., 2006; Tejado et al., 2007), a suggested main reaction mechanism in the cellulose fibers/MPU-20 blends during steam injection process is the following (as shown in Scheme 1):

During steam injection process, some of the —NCO groups of MPU-20 resin in contact with cellulose fibers reacted with —OH groups of the cellulose fibers under the high temperature of the steam, which resulted in the formation of urethane groups (—NH—CO—O—) forming between cellulose fibers. Simultaneously, other —NCO groups in the MPU-20 resin, but not in contact with

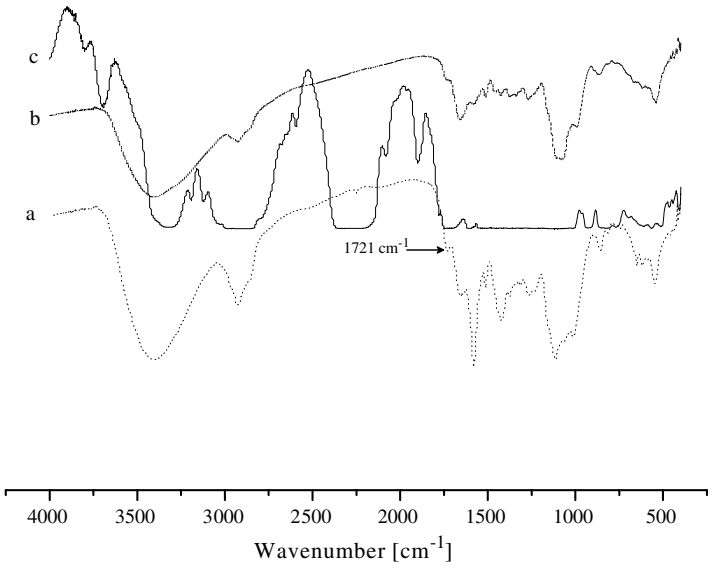

Fig. 3. FTIR spectra of CFMCs (a), cellulose fibers (b) and MPU-20 (c).

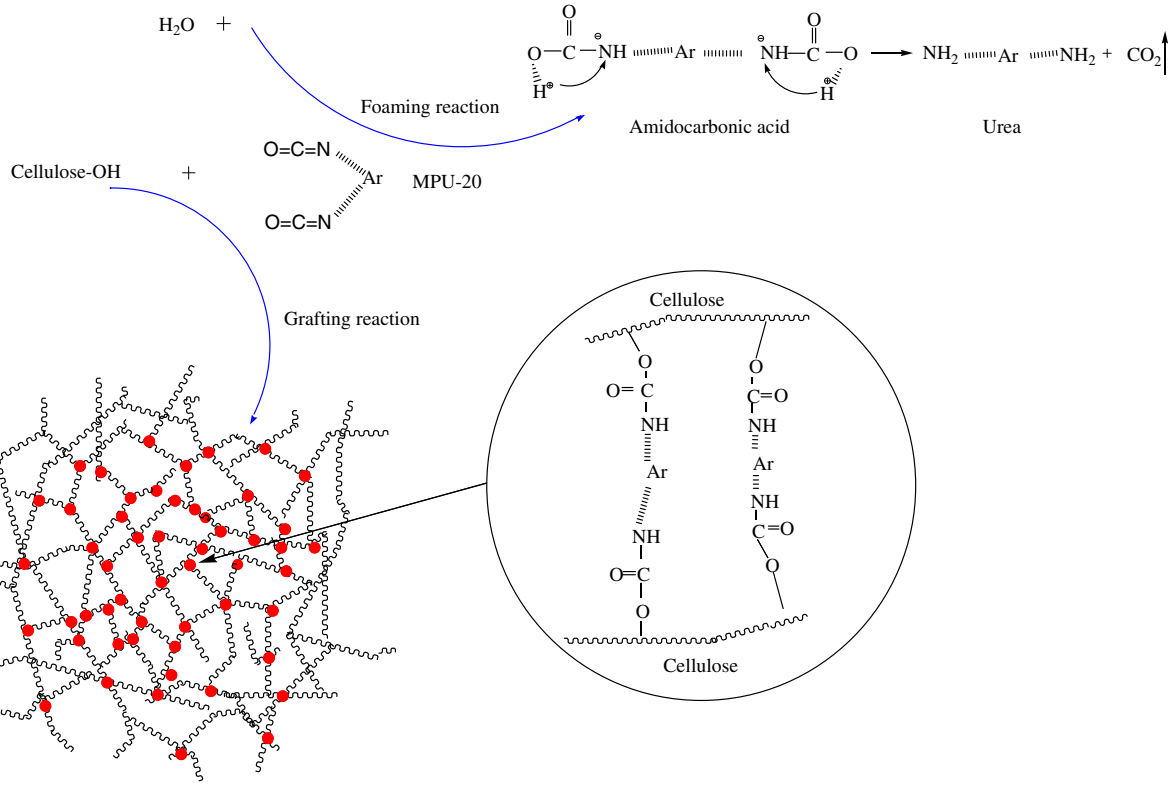

Scheme 1. Proposed main two reaction mechanisms including grafting reactions and foaming reactions in the cellulose fibers/MPU-20 blends during steam injection process.

cellulose fibers, reacted with the water vapor to produce carbon dioxides in the foaming reactions, which expanded the between-fibers voids. It is these foaming reactions and grafting reactions during steam injection process in cellulose fibers/MPU-20 blends that give the CFMCs composites their special physical structures and cushioning properties.

3.2. Cushion properties analysis

Compressive stress-strain and cushion factor-strain curves were investigated as a function of steam injection pressure, transmission time, holding time, MPU-20 dosage and apparent specific gravity. The results are shown in Figs. 4–8.

As can be seen from the experimental results of the compressive stress-strain curves, there were almost two compression stages in the compressive process. Firstly, stress increased gradually or even linearly with the increase of strain, and subsequently increased sharply with a further increase in strain. There were always two short yield deformation stages in the compressive process (as shown in Fig. 4), in which there was nearly no increase or even a decrease in stress with the increasing strain.

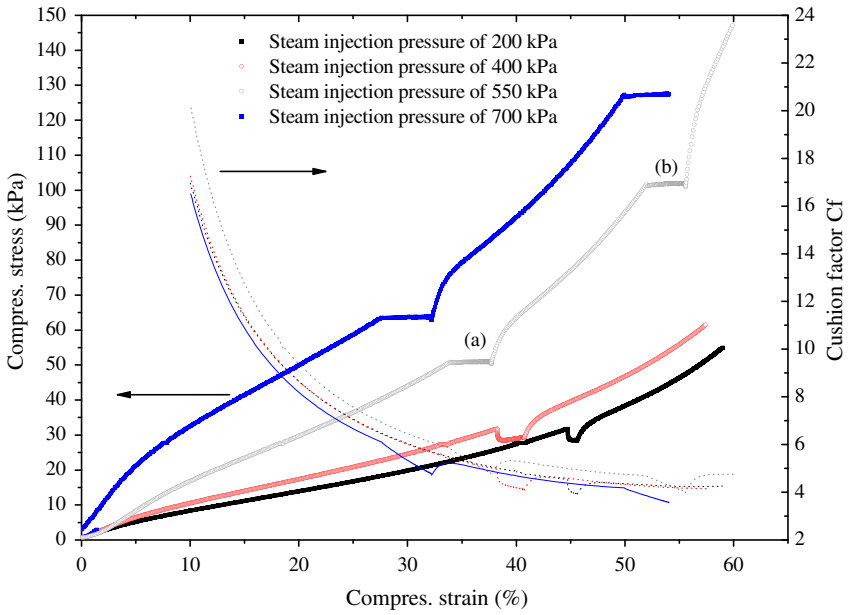

Fig. 4. The experimental effects of steam injection pressure on static mechanical properties for the CFMCs samples: (a) First yield deformation stage; (b) Second yield deformation stage.

A possible mechanism for the two yield deformation stages seen in compressive stress-strain curves is the following: (as shown in Scheme 2).

In stage (1), the stress increase with increasing of strain, is likely to be the result of the compression of the void cells in void bodies; In stage (2), the short yield deformation stages shows the void cavities of void bodies begin being compressed, bruised and approximately changed into the compressed void cells structure after the void cells were compressed to a certain degree. The first yield deformation stage in the compression process is probably associated with the part void cavities in locations adjacent to the samples' surfaces and which are initially compressed. As the compressive strain increases further, the void cells adjacent to core locations of the samples also start to be compressed, which starts the process of stress increasing with strain between the two yield deformation stages. When void cells adjacent to core locations of the samples are compressed to a certain degree, the void cavities in the void bodies adjacent to the core locations begin to be compressed as above, which indicates the second yield deformation stage in the compression process. In the end, nearly all the void cavities in void bodies of the samples are compressed and bruised, and subsequently the whole compressed void cells begin being compressed as the further increase of compressive strain in Stage (3), which shows that the densifications of the compressed void cells cause the sharp increase in compressive stress as the strain increases further.

When steam was injected, water vapor moved quickly through the cellulose fibers/MPU-20 blends as a result of external pressure gradients. During complex physical and chemical reactions occurred. Increasing steam injection pressure increases the blend temperature. At constant apparent specific gravity of 80 kg/m^3, MPU-20 dosage of 20%, transmission time of 10 s and holding time of 7 min, Fig. 4 suggested that increasing steam injection pressure can increase stress under the same strain, and also the first yield deformation stage is shifted to the left or occurred at lower strain location with increasing steam injection pressures. The results indicated that higher steam injection pressure was desirable for improving the cushioning properties due to the lower cushion factor achieved compared to the other steam injection pressures. Generally, the cushion materials with low cushion factors are

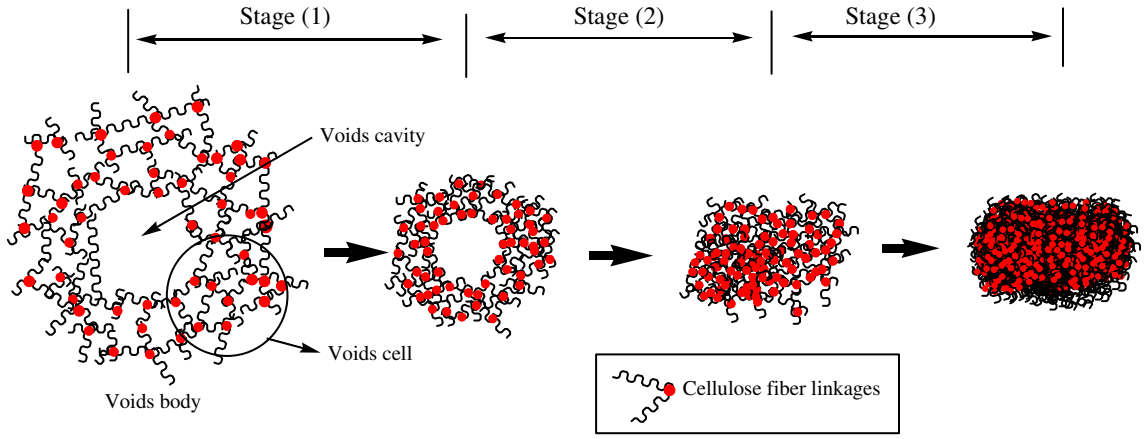

Scheme 2. Ideal model for describing the deformations of void units in compressive process in response to compressive stress–compressive strain curves.

recommended for the cushion design. Cushion factor of the CFMCs samples moulded by steam injection pressure at 700 kPa was the lowest at 55% strain (as shown in Fig. 4).

Fig. 5 suggested longer transmission time resulted in lower stress or higher cushion factors, when subjected to the same strain under constant apparent specific gravity of 80 kg/m^3, MPU-20 dosage of 20%, steam injection pressure of 600 kPa and holding time of 10 min. This observation can be understood as being a result of poor bonding between cellulose fibers or excessive thermal decompositions of the cellulose fibers. When the application of steam was terminated, residual physical changes (thermal decompositions) and chemical reactions (foaming and grafting reactions) were still in progress as the cellulose fibers/MPU-20 blends were held in the former. As we can see from Fig. 6, at constant apparent specific gravity of 80 kg/m^3, MPU-20 dosage of 20%, steam injection pressure of 700 kPa and transmission time of 10 s, using longer holding time resulted in lower stress or higher cushion factors when subject to the same strain, which probably resulted from the thermal decomposition of cellulose and hemi-cellulose.

Foam-type polyurethane resin of MPU-20 plays a very important role in the preparation of the CMFCs. At constant apparent specific gravity of 80 kg/m^3, holding time of 10 min, steam injection pressure of 600 kPa and transmission time of 10 s, increasing MPU-20 dosage increased stress or decreased cushion factors at the same strain (as shown in Fig. 7), which probably resulted from better bonding between cellulose fibers and more or larger voids in the structure. The apparent specific gravity of the CFMCs has obvious effects on cushion properties, and increasing apparent specific gravity increased stress at the same strain under constant MPU-20 dosage of 20%, holding time of 10 min, steam injection pressure of

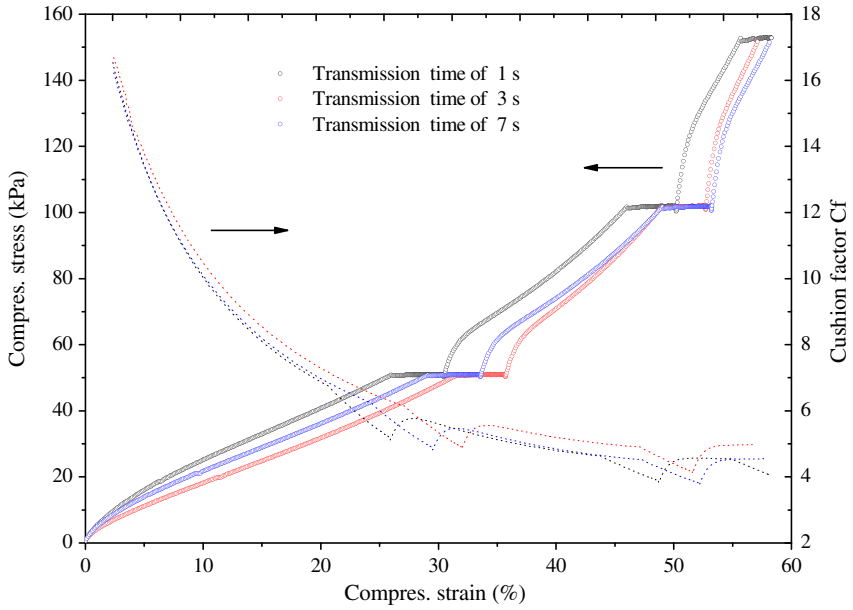

Fig. 5. The experimental effects of steam transmission time on static compression properties for the CFMCs samples.

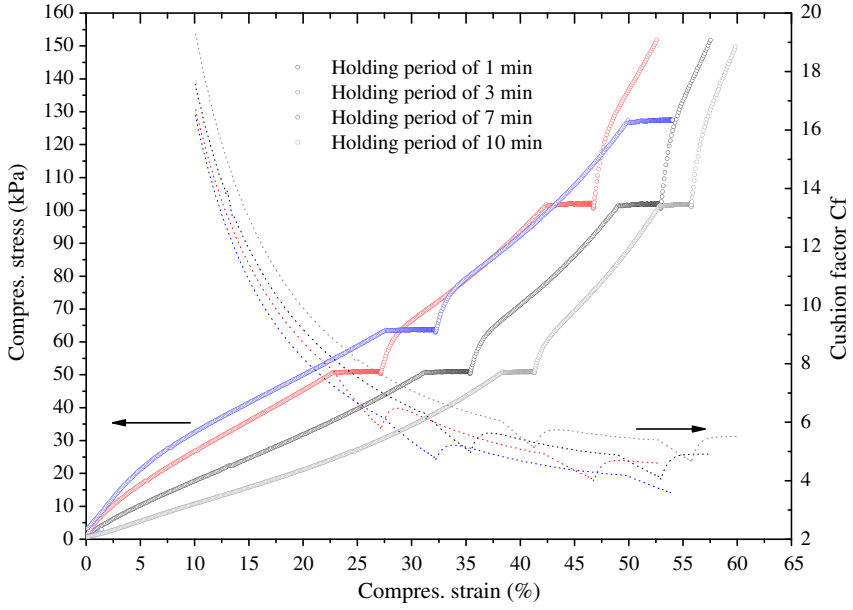

Fig. 6. The experimental effects of holding time on static compression properties for the CFMCs samples.

550 kPa and transmission time of 10 s. However, the apparent specific gravity determines the porosity of porous blends (Dai, Yu, & Zhou 2005). Higher apparent specific gravities of the samples reflected fewer voids in the structure, and resulted in poorer cushioning properties. This situation can be seen from Fig. 8, which indicated that the lowest cushioning factor for the CFMCs samples of 70 kg/m^3, which was lower than the cushioning factor observed in the 100 kg/m^3. Hence, the CFMCs with apparent specific gravity of 70 kg/m^3 had the best cushioning properties observed in this study.

As a result, the experimental results showed that cellulose fibers/MPU-20 composites (CFMCs) with apparent specific gravity lower than 100 kg/m^3 and thickness of 20–200 mm has been successfully manufactured by self-designed steam injection technology and equipment. The CFMCs are soft and elastic (as shown in Fig. 9). The CFMCs have lower compressive stress than EPS, moulded pulp or corrugated board at the same compressive strain (Noguchi et al., 1997). Further, it has also good cushioning properties, with cushion factors lower than 4. These data indicate that the CFMCs can perform well in uses such as packaging smaller electric products. In addition, the CFMCs were biodegradable and cost-competitive. Any fungi on cellulose fibers would be killed by the steam treatment at high temperature, which would looked upon favorably by quarantine departments involved with exporting or importing packaged products. A moulded sample of the CFMCs can be released from the former after total cycle time of 1.5 min, which includes a transmission time of 1 s, penetration time of 10–30 s and holding time of 1 min. Note that the values of these

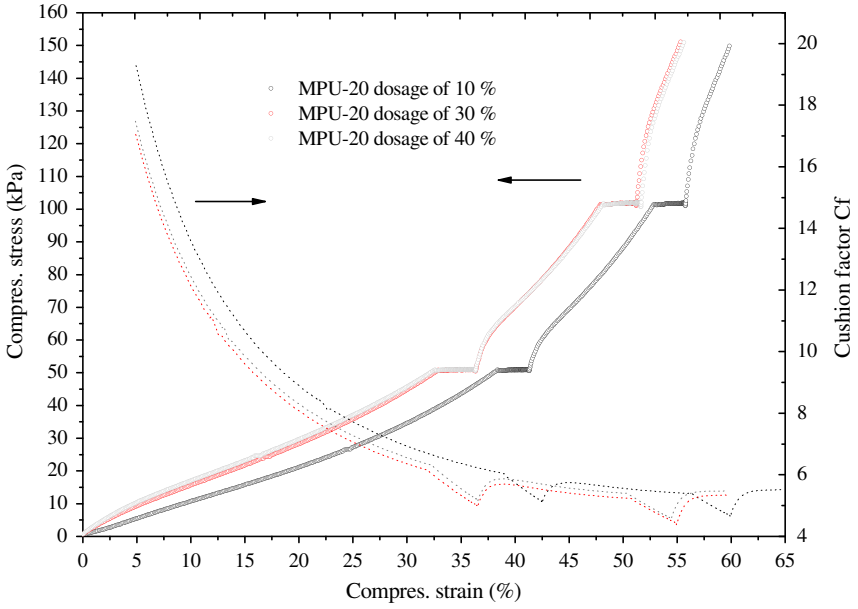

Fig. 7. The experimental effects of MPU-20 dosage on static compression properties for the CFMCs samples.

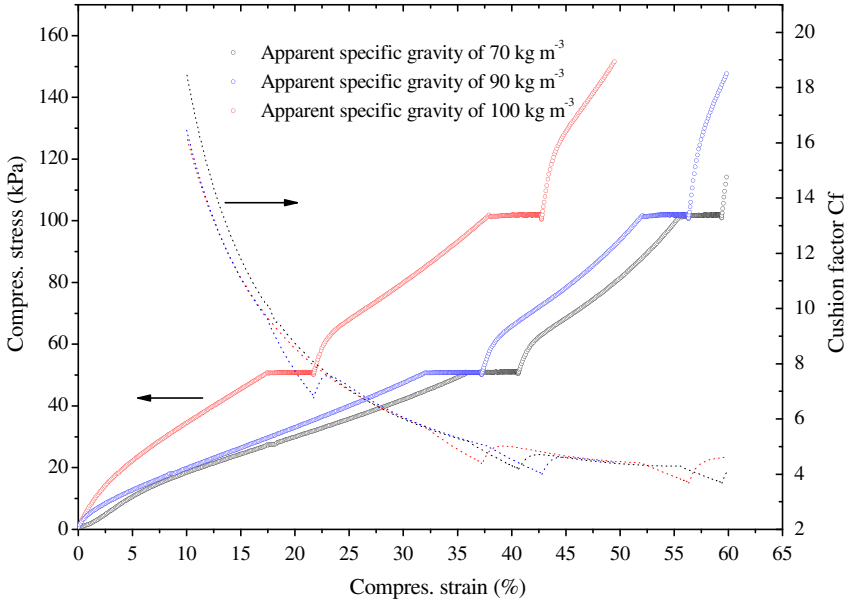

Fig. 8. The experimental effects of apparent specific gravity on static compression properties for the CFMCs samples.

parameters are all approximately the same as that achieved in the production of moulded pulp packaging material or styrene foam (Noguchi et al., 1997).

3.3. X-ray diffraction (XRD) analysis

XRD has been used extensively for the investigations of the supramolecular order (cristallinity) of cellulose fibers and their derivatives. Fig. 10 showed the XRD curves of CFMCs sample, as well as the cellulose fibers blends untreated and treated by steam injection treatment. It was found that the main diffraction signals at 2θ values were 15.2°, 15.88°, 22.52° and 34.6°, which are normally assigned to the diffraction planes 101, $10\bar{1}$, 002, and 040, respectively. Compared to untreated cellulose fiber blends, it was observed that the major diffraction intensities for the cellulose fibers blends treated by steam injection and the corresponding CFMCs appearing around at 15.2°, 15.88°, 22.52° were less intense and shifted to a higher 2θ value, These data indicate that cellulose fibers treatment had damaged the crystalline structures of cellulose fibers. Compared to the cellulose fibers blends treated by steam injection, however, diffraction intensity of the CFMCs at 2θ of 15.88° by crystalline planes $10\bar{1}$ was observed. This observation suggested that the grafting reactions between —NCO groups from MPU-20 and hydroxyl groups from cellulose fibers involved the hydroxyl groups in the crystalline regions of the deeper layers of cell walls except for the hydroxyl groups belonging to the outer layers of the cell walls.

3.4. DTA/TGA analysis

The thermogravimetric curves are shown in Fig. 11 for the cellulose fibers blends untreated and treated by steam injection treatment and for the CFMCs. The weight losses of the above samples in an oxygen atmosphere occurring in the range from room temperature (30 °C) to 150 °C was 5.73%, 7.63% and 5.62%, respectively, due to the elimination of absorbed or combined water (Tomczak, Satyanarayana, & Sydenstricker, 2007). The greatest decomposition of cellulose fibers blends untreated and treated and the CFMCs occurred at temperature (T_d) 323 °C, 318 °C and 291 °C, respectively. The combined weight loss from 150 °C to T_d was 40.23%, 38.75% and 23.1% for above samples, which resulted from the thermal degradation of cellulose, semi-cellulose and lignin. The decreased T_d for cellulose fibers blends treated by steam injection indicated that the steam injection treatments accelerated thermal decomposition of cellulose fiber constituents. Compared to cellulose fibers untreated and treated by steam injection, however, the CFMCs had

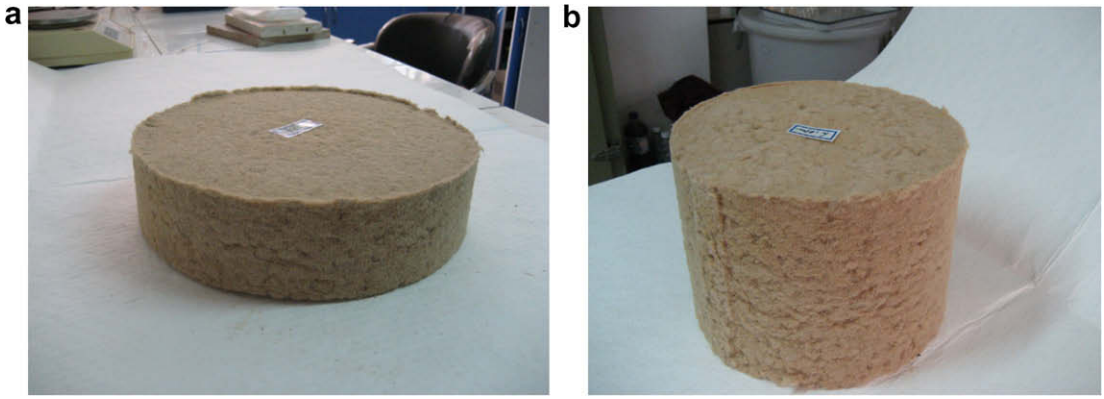

Fig. 9. The moulded CFMCs samples with apparent specific gravity of 80 kg/m^3 and thicknesses of 50 mm (a) and 150 mm (b).

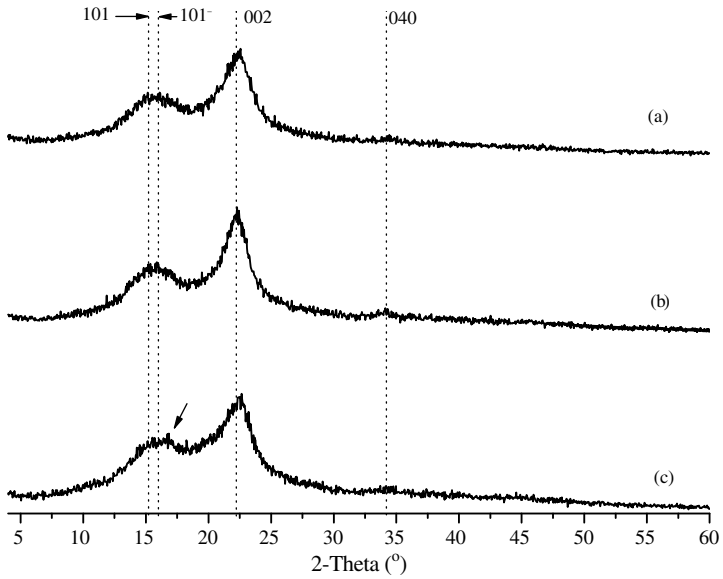

Fig. 10. XRD patterns of cellulose fibers treated (a), cellulose fibers untreated (b) and the CFMCs (c).

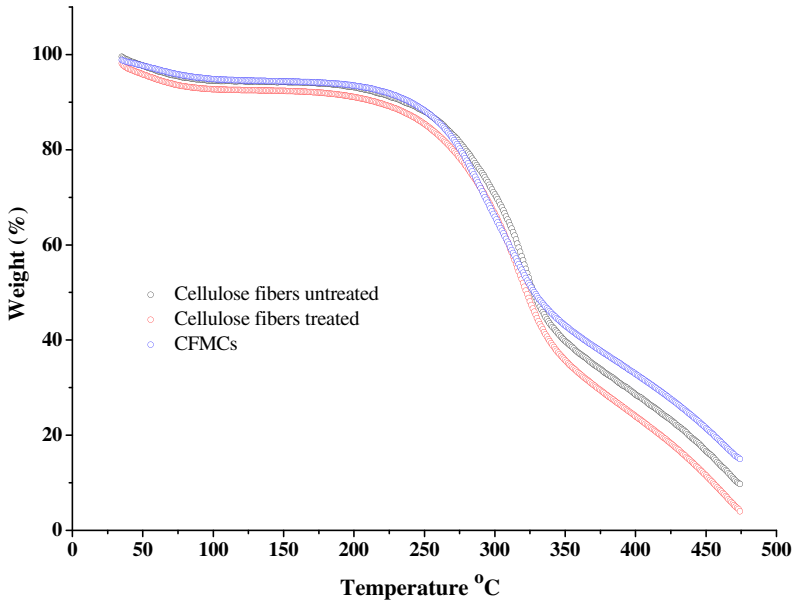

Fig. 11. Temperature dependences of weight loss for treated and untreated cellulose fibers by steam injection, cellulose fibers untreated and the CFMCs in an oxygen atmosphere.

less weight loss in the degradation process. This observation suggests that the CFMCs has better thermal stability due to better cellulose fiber bonding, simply more thermal resistant materials.

Fig. 12 showed DTA curves of cellulose fibers untreated and treated by steam injection and the CFMCs used in this study. The DTA peaks of the above samples in an oxygen atmosphere clearly indicated that their decompositions were mainly exothermic, but minor endothermic peaks were also observed in the initial degradation stage, especially for the cellulose fibers treated by steam injection. Two exothermic peaks indicated oxidative pyrolysis of cellulose and fall out of side groups (around 330 °C), and oxidative combustion of carbon residue (around 470 °C) (Zhang, Rong, & Lu, 2005). Another minor exothermic peak at 302 °C was observed in the CFMCs, which may be attributed to oxidation of the CFMCs and also separations of urethane from cellulose.

3.5. Morphology analysis

The scanning electron micrographs of the fracture surfaces of cellulose fibers blends before and after steam injection treatment are shown in Fig. 13. The micrographs clearly show that the surfaces of the cellulose fibers are rough after steam injection treatment. There were some slight troughs on the surfaces of the cellulose fibers subjected to steam injection, which probably resulted from the thermal or hydrolytic decompositions of cellulose, hemi-cellulose and lignin. It should be noted that, the increase in external roughness of cellulose fibers after steam injection treatment is beneficial for improving bonding by providing a greater effective surface area available for bonding. It can be seen in Fig. 14 that there were several small resin particles distributed around and/or on the surface of cellulose fibers. It is these resin

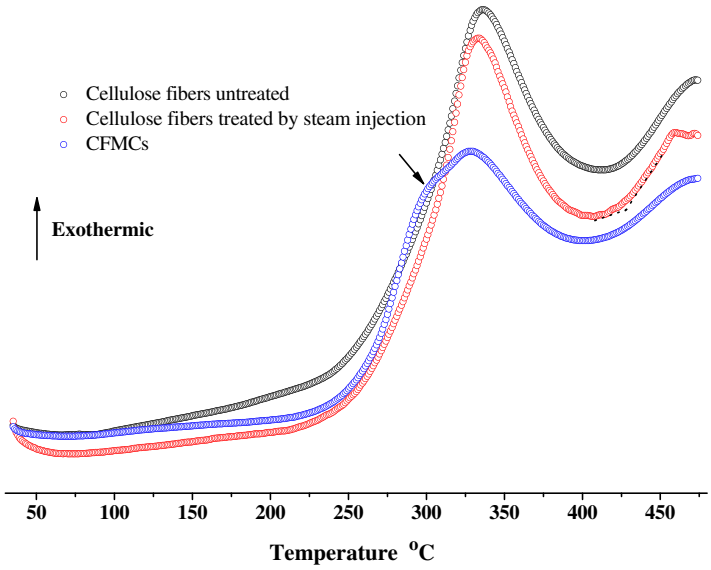

Fig. 12. DTA curves for cellulose fibers untreated and treated by steam injection, and the CFMCs in oxygen atmosphere.

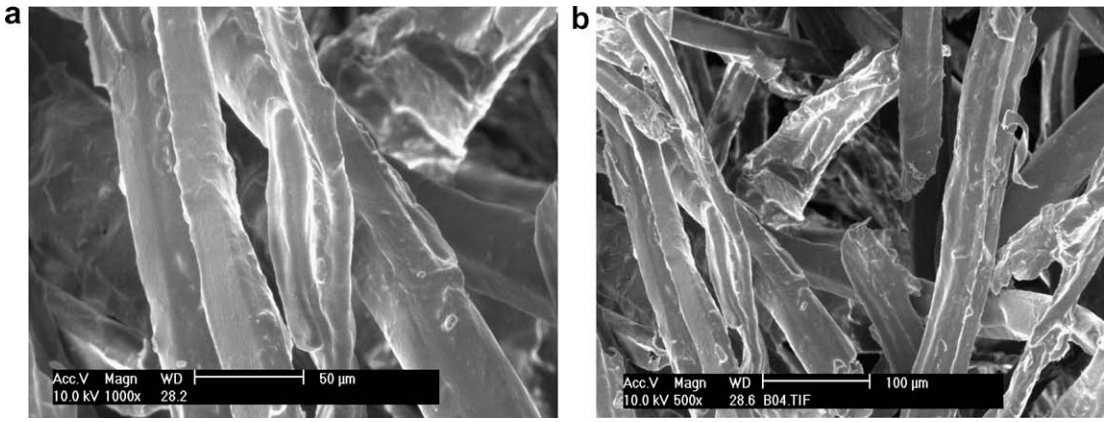

Fig. 13. SEM micrographs of fracture surfaces of cellulose fibers blends: (a) before steam injection treatment; (b) after steam injection treatment.

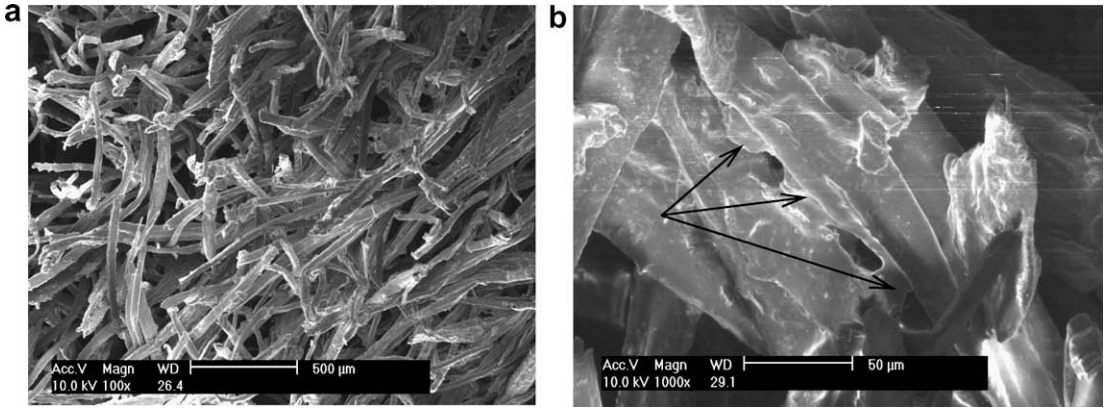

Fig. 14. SEM micrographs of CFMCs samples: (a) overall observation for the CFMCs sample; (b) ultra-microstructure in cellulose fiber–cellulose fiber.

particles that bond the cellulose fibers together. The MPU-20 resin particles are theoretically divided into two parts: One part of the MPU-20 resin particles are distributed on the contacting surfaces between cellulose fibers and are mainly engaged in the grafted reactions; The other part of the MPU-20 resin particles are distributed on the non-contact surfaces between cellulose fibers and are mainly engaged in the foaming reactions as water vapor moves in the voids. The ultra-microstructure of a single cellulose fiber and fiber-resin particle- fiber were further studied by atomic force microscopy (AFM) with the results displayed in Fig. 15. It was observed that microfibrils were arranged regularly in a cellulose fiber (as shown in Fig. 15a). In contrast, the ultra-microstructures in the fiber-resin particle-fiber were complex, and the shapes of resin particles located between cellulose fibers can be described as form-

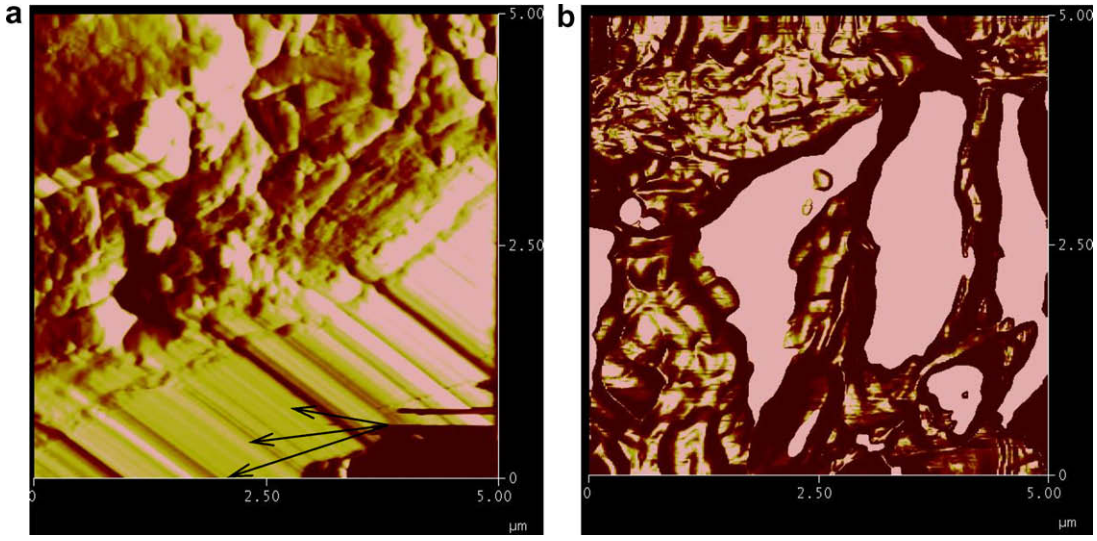

Fig. 15. AFM micrographs of detailed ultra-microstructure of single fiber (a) and cellulose fiber-resin particle–cellulose fiber (b).

ing cross connections, which are indicated with the special shapes of "X" by smaller in middle zone and larger on the two ends (as shown in Fig. 15b).

4. Conclusions

In this study the moulded cellulose fibers/MPU-20 composites (CFMCs) with apparent specific gravity lower than 100 kg/m^3 and thickness of 20–200 mm have been successfully manufactured using self-designed steam injection technology and equipment. Compressive stress-strain curves indicated there were two stages in the compressive process: A region in which stress gradually increased with the increase of strain, followed by a region in which the stress increased rapidly in response to further increase in strain. The cushioning properties of the CFMCs, improved with higher steam injection pressures and higher MPU-20 dosages. Appropriate transmission times, holding times and the CFMCs apparent specific gravities were suggested as a result of this work. After steam injection treatment, the cellulose fibers surface became rough, which was a desirable feature leading to enhanced bondable surface area. It was observed by AFM analysis that shapes of resin particles located between cellulose fibers can be described by the "X" by being smaller in middle zone and larger at the two ends. An absorption peak at 1721 cm^{-1} was observed by FTIR analysis that is attributable for the formation of urethane (—NH—CO—O—) resulting from the reactions between —NCO groups of the MPU-20 resin and —OH groups in the cellulose fibers. The hydroxyl groups belonging to crystalline regions were also involved in the above chemical reactions exception for the amorphous regions. In addition, it was observed that steam injection treatment degraded the crystalline structure. Compared to cellulose fibers blends untreated and treated by steam injection, the CFMCs have less weight loss in the thermal degradation process but a lower decomposition temperature. The degradation process of the cellulose fibers and the CFMCs in an oxygen atmosphere were mainly exothermic, with two exothermic peaks that were attributed to oxidative pyrolysis of cellulose fibers loss of side groups (around 330 °C) and oxidative combustion of carbon residues (around 470 °C), respectively. Although the CFMCs have lower stress than EPS or moulded pulp at the same strain, improved cushioning properties are seen with cushion factors lower than 4 and also the yield deformation stages in compressive process. A moulded sample of the composite can be released from the former after total cycle time of 1.5 min, including transmission time of 1 s, penetration time of 10–30 s and holding time of 1 min. Moreover, the CFMCs, which are biodegradable and cost-competitive, can be also used as a new composite for cushioning small electrical products.

Acknowledgements

Many thanks for the support provided by Guangdong Public Laboratory of Paper Technology and Equipment and State Key Laboratory of Pulp and Paper Engineering in South China University of Technology in China. During the preparation of the manuscript, the authors benefited from helpful discussions with Dr. Donald G. Barnes, Visiting Professor of Chemistry at Guangxi University, Nanning, Guangxi Zhuang Autonomous Region, People's Republic of China.

References

Avella, M., Vlieger, J. D., Errico, M. E., Fischer, S., Vacca, P., & Volpe, M. G. (2005). Biodegradable starch/clay nanocomposite films for food packaging applications. *Food Chemistry, 93*(3), 467–474.

Bourmaud, A., & Baley, C. (2007). Investigations on the recycling of hemp and sisal fibre reinforced polypropylene composites. *Polymer Degradation and Stability, 92*(6), 1034–1045.

Chang, C. P., & Hung, S. C. (2003). Manufacture of flame retardant foaming board from waste papers reinforced with phenol–formaldehyde resin. *Bioresource Technology, 86*(2), 201–202.

Dai, C. P., Yu, C. M., & Zhou, X. Y. (2005). Heat and mass transfer in wood composite panels during hot-pressing, part II: modeling void formation and mat permeability. *Wood and Fiber Science, 37*, 242–257.

Das, S., Malmberg, M. J., & Frazier, C. E. (2007). Cure chemistry of wood/polymeric isocyanate (PMDI) bonds: Effect of wood species. *International Journal of Adhesion and Adhesives, 27*, 250–257.

Gironès, J., Pimenta, M. T. B., Vilaseca, F., Carvalho, A. J. F., Mutjé, P., & Curvelo, A. A. S. (2007). Blocked isocyanates as coupling agents for cellulose-based composites. *Carbohydrate Polymers, 68*(3), 537–543.

Guan, J. J., Eskridge, K. M., & Hanna, M. A. (2005). Acetylated starch-polylactic acid loose-fill packaging materials. *Industrial Crops and Products, 22*(2), 109–123.

Hata, T. (1993). Heat flow in particle mat and properties of particleboard under steam-injection pressing. Ph.D. thesis, Kyoto University, Japan, 1993, pp. 1–47.

Karmarkar, A., Chauhan, S. S., Modak, J. M., & Chanda, M. (2007). Mechanical properties of wood fiber reinforced polypropylene composite: Effect of a novel compatibilizer with isocyanate functional group. *Composites, Part A: Applied Science and Manufacturing, 38*(2), 227–233.

Kawasaki, T., Zhang, M., & Kawai, S. (1998). Manufacture and properties of ultra-low-density fiberboard. *Journal Wood Science, 44*, 354–360.

Lui, W. B., & Peng, J. (2007). Effects of initial load levels and crosshead speed levels on viscoelastic properties of biodegradable loose fill extrudates. *Journal of Food Engineering, 80*(1), 284–291.

Mohanty, A. K., Wibowo, A., Misra, M., & Drzal, L. T. (2004). Effect of process engineering on the performance of natural fiber reinforced cellulose acetate biocomposite. *Composties, Part A: Applied Science and Manufacturing, 35*(3), 363–370.

Mugnozza, G. S., Schettini, E., Vox, G., Malinconico, M., Immirzi, B., & Pagliara, S. (2006). Mechanical properties decay and morphological behaviour of biodegradable films for agricultural mulching in real scale experiment. *Polymer Degradation and Stability, 91*(11), 2801–2808.

Noguchi, T., Miyashita, M., Seto, J., Tan, M., & Kawano, M. (1997). Development of moulded pulp materials for the packaging of electronic equipment. *Packaging Technology and Science, 10*, 161–168.

Silva, A. L. D., Martínez, J. M. M., & Bordado, J. C. M. (2006). Influence of the free isocyanate content in the adhesive properties of reactive trifunctional polyether urethane quasi-prepolymers. *International Journal of Adhesion and Adhesives, 26*(5), 355–362.

Steinbüchel, A. (1992). Biodegradable plastics. *Current Opinion in Biotechnology, 3*(3), 291–297.

Tatarka, P. D., & Cunningham, R. L. (1998). Properties of protective loose-fill foams. *Journal of Polymer Science, 67*(7), 1157–1176.

Tejado, A., Kortaberria, G., Peña, C., Labidi, J., Echeverria, J. M., & Mondragon, I. (2007). Isocyanate curing of novolac-type lingo–phenol–formaldehyde resins. *Industrial Crops and Products*. doi:10.1016/j.indcrop.2007.07.00.

Tomczak, F., Satyanarayana, K. G., & Sydenstricker, T. H. D. (2007). Studies on lignocellulosic fibers of Brazil: Part III – morphology and properties of Brazilian curauá fibers. *Composites, Part A: Applied Science and Manufacturing*. doi:10.1016/j.compositesa.2007.06.00.

Voorn, B. V., Smit, H. H. G., Sinke, R. J., & Klerk, B. D. (2001). Natural fibre reinforced sheet moulding compound. *Composites, Part A: Applied Science and Manufacturing, 32*(9), 1271–1279.

Vox, G., & Schettini, E. (2007). Evaluation of the radiometric properties of starch-based biodegradable films for crop protection. *Polymer Testing, 26*(5), 639–651.

Widyorini, R., Xu, J. Y., Watanabe, T., & Kawai, S. (2005). Chemical changes in steam-pressed kenaf core binderless particleboard. *Journal Wood Science, 51*(11), 26–32.

Yogaraj, N., & Ramani, N. (2006). Twin-screw extrusion production and characterization of starch foam products for use in cushioning and insulation applications. *Polymer Engineering and Science, 46*, 438–451.

Zhang, M. Q., Rong, M. Z., & Lu, X. (2005). Fully biodegradable natural fiber composites from renewable resources: All-plant fiber composites. *Composites Science and Technology, 65*(15), 2514–2525.